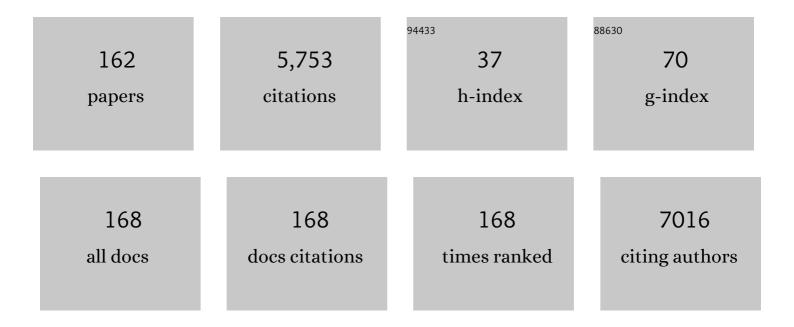
List of Publications by Year in descending order

Source: https://exaly.com/author-pdf/7836166/publications.pdf Version: 2024-02-01



YUWAL COLAN

#	Article	IF	CITATIONS
1	The role of interparticle and external forces in nanoparticle assembly. Nature Materials, 2008, 7, 527-538.	27.5	1,049
2	Assessment of carrier-multiplication efficiency in bulk PbSe and PbS. Nature Physics, 2009, 5, 811-814.	16.7	245
3	Vacuum-deposited gold films. Surface Science, 1992, 264, 312-326.	1.9	168
4	New Nanocrystalline Materials: A Previously Unknown Simple Cubic Phase in the SnS Binary System. Nano Letters, 2015, 15, 2174-2179.	9.1	126
5	Synthesis and properties of nanocrystalline π-SnS – a new cubic phase of tin sulphide. RSC Advances, 2016, 6, 5848-5855.	3.6	124
6	Superior Biolubricant from a Species of Red Microalga. Langmuir, 2006, 22, 7313-7317.	3.5	112
7	A Semiconductor-Nanowire Assembly of Ultrahigh Junction Density by the Langmuir-Blodgett Technique. Advanced Materials, 2006, 18, 210-213.	21.0	109
8	Structural and optical properties of GaN laterally overgrown on Si(111) by metalorganic chemical vapor deposition using an AlN buffer layer. MRS Internet Journal of Nitride Semiconductor Research, 1999, 4, 1.	1.0	107
9	Raman Spectroscopy of Ultranarrow CdS Nanostructures. Journal of Physical Chemistry C, 2007, 111, 11843-11848.	3.1	104
10	The Effect of Growth Environment on the Morphological and Extended Defect Evolution in GaN Grown by Metalorganic Chemical Vapor Deposition. Japanese Journal of Applied Physics, 1998, 37, 4460-4466.	1.5	101
11	Synthesis, Two-Dimensional Assembly, and Surface Pressure-Induced Coalescence of Ultranarrow PbS Nanowires. Nano Letters, 2007, 7, 1459-1462.	9.1	100
12	Epitaxial electrodeposition of cadmium selenide nanocrystals on gold. Langmuir, 1992, 8, 749-752.	3.5	97
13	Structural Transitions in Polydiacetylene Langmuir Films. Langmuir, 2009, 25, 4469-4477.	3.5	90
14	A Bottom-Up Approach toward Fabrication of Ultrathin PbS Sheets. Nano Letters, 2013, 13, 409-415.	9.1	90
15	Microtribology and Direct Force Measurement of WS2 Nested Fullerene-Like Nanostructures. Advanced Materials, 1999, 11, 934-937.	21.0	83
16	Ultra Narrow PbS Nanorods with Intense Fluorescence. Journal of the American Chemical Society, 2008, 130, 4594-4595.	13.7	83
17	Synthesis, Assembly, and Optical Properties of Shape- and Phase-Controlled ZnSe Nanostructures. Langmuir, 2007, 23, 765-770.	3.5	82
18	Switchable Assembly of Ultra Narrow CdS Nanowires and Nanorods. Journal of the American Chemical Society, 2006, 128, 9294-9295.	13.7	80

#	Article	IF	CITATIONS
19	Crystal structure of a large cubic tin monosulfide polymorph: an unraveled puzzle. CrystEngComm, 2016, 18, 5188-5194.	2.6	76
20	Frictional Properties of Confined Nanorods. Advanced Materials, 2006, 18, 2589-2592.	21.0	74
21	Shape-Dependent Confinement in Ultrasmall Zero-, One-, and Two-Dimensional PbS Nanostructures. Journal of the American Chemical Society, 2009, 131, 11282-11283.	13.7	73
22	Origin of the Contact Angle Hysteresis of Water on Chemisorbed and Physisorbed Self-Assembled Monolayers. Langmuir, 2012, 28, 14609-14617.	3.5	68
23	Microtribology and Friction-Induced Material Transfer in WS2 Nanoparticle Additives. Advanced Functional Materials, 2001, 11, 348-354.	14.9	64
24	Electrodeposited quantum dots. Surface Science, 1994, 311, L633-L640.	1.9	60
25	Polarization Properties and Switchable Assembly of Ultranarrow ZnSe Nanorods. Advanced Materials, 2007, 19, 1105-1108.	21.0	60
26	Morphology and microstructural evolution in the early stages of hydride vapor phase epitaxy of GaN on sapphire. Applied Physics Letters, 1998, 73, 3090-3092.	3.3	59
27	Atomic Positional Versus Electronic Order in Semiconducting ZnSe Nanoparticles. Physical Review Letters, 2009, 103, 136802.	7.8	59
28	A new nanocrystalline binary phase: synthesis and properties of cubic tin monoselenide. CrystEngComm, 2016, 18, 1918-1923.	2.6	59
29	Electrodeposited Quantum Dots. 3. Interfacial Factors Controlling the Morphology, Size, and Epitaxy. The Journal of Physical Chemistry, 1996, 100, 2220-2228.	2.9	57
30	Adhesion and Stable Low Friction Provided by a Subnanometer-Thick Monolayer of a Natural Polysaccharide. Langmuir, 2008, 24, 1534-1540.	3.5	56
31	EPITAXY and orientation control in chemical solution deposited PbS and PbSe monocrystalline films. Journal of Crystal Growth, 2007, 304, 169-178.	1.5	48
32	Forces between Surfaces across Nanoparticle Solutions:Â Role of Size, Shape, and Concentration. Langmuir, 2007, 23, 3961-3969.	3.5	47
33	The role of solution composition in chemical bath deposition of epitaxial thin films of PbS on GaAs(100). Journal of Crystal Growth, 2007, 308, 334-339.	1.5	44
34	Direct Observation of Shear-Induced Orientational Phase Coexistence in a Lyotropic System Using a Modified X-Ray Surface Forces Apparatus. Physical Review Letters, 2001, 86, 1263-1266.	7.8	42
35	Size shift of XPS lines observed from PbS nanocrystals. Surface and Interface Analysis, 2010, 42, 850-854.	1.8	42
36	Hierarchical Assembly of Ultranarrow Alkylamine-Coated ZnS Nanorods: A Synchrotron Surface X-Ray Diffraction Study. Nano Letters, 2008, 8, 3858-3864.	9.1	39

#	Article	IF	CITATIONS
37	A new cubic prototype structure in the IV–VI monochalcogenide system: a DFT study. CrystEngComm, 2017, 19, 1751-1761.	2.6	39
38	Electrochemical characterization and morphological studies of palladium-modified carbon ceramic electrodes. Journal of Electroanalytical Chemistry, 1995, 395, 57-66.	3.8	38
39	Forces between Surfactant-Coated ZnS Nanoparticles in Dodecane: Effect of Water. Advanced Functional Materials, 2006, 16, 2127-2134.	14.9	36
40	Reaction of Alkylamine Surfactants with Carbon Dioxide: Relevance to Nanocrystal Synthesis. Nano Letters, 2009, 9, 2088-2093.	9.1	36
41	Microstructure and morphology evolution in chemical solution deposited PbSe films on GaAs(100). EPJ Applied Physics, 2003, 24, 13-20.	0.7	35
42	Chemically deposited PbSe thin films: factors deterring reproducibility in the early stages of growth. CrystEngComm, 2014, 16, 10553-10559.	2.6	35
43	Controlled Deposition of Oriented PbS Nanocrystals on Ultrathin Polydiacetylene Templates at the Airâ^'Solution Interface. Langmuir, 2003, 19, 10962-10966.	3.5	34
44	The Temperature-Dependent Structure of Alkylamines and Their Corresponding Alkylammonium-Alkylcarbamates. Journal of the American Chemical Society, 2009, 131, 9107-9113.	13.7	34
45	A comparative study of the structure and optical properties of copper sulfide thin films chemically deposited on various substrates. RSC Advances, 2013, 3, 23066.	3.6	34
46	Chemical epitaxy of semiconductor thin films. MRS Bulletin, 2010, 35, 790-796.	3.5	33
47	Phase transition kinetics in Langmuir and spin-coated polydiacetylene films. Physical Chemistry Chemical Physics, 2010, 12, 713-722.	2.8	33
48	Epitaxial size control by mismatch tuning in electrodeposited Cd(Se, Te) quantum dots on {111} gold. Advanced Materials, 1996, 8, 631-633.	21.0	32
49	Nanocrystalline Ag2S on Polydiacetylene Langmuir Films. Crystal Growth and Design, 2005, 5, 439-443.	3.0	31
50	Oneâ€Pot Hydrothermal Synthesis of Elements (B, N, P)â€Doped Fluorescent Carbon Dots for Cell Labelling, Differentiation and Outgrowth of Neuronal Cells. ChemistrySelect, 2019, 4, 4222-4232.	1.5	29
51	Chemically deposited PbS thin film photo-conducting layers for optically addressed spatial light modulators. Journal of Materials Chemistry C, 2014, 2, 9132-9140.	5.5	28
52	Dynamics of Hydration of Nanocellulose Films. Advanced Materials Interfaces, 2016, 3, 1500415.	3.7	28
53	Role of sonication pre-treatment and cation valence in the sol-gel transition of nano-cellulose suspensions. Scientific Reports, 2017, 7, 11129.	3.3	28
54	In situ imaging of shearing contacts in the surface forces apparatus. Wear, 2000, 245, 190-195.	3.1	27

#	Article	IF	CITATIONS
55	Microstructure and morphology evolution in chemically deposited semiconductor films: 4. From isolated nanoparticles to monocrystalline PbS thin films on GaAs(100) substrates. EPJ Applied Physics, 2007, 37, 39-47.	0.7	27
56	Ï€â€Phase Tin and Germanium Monochalcogenide Semiconductors: An Emerging Materials System. Advanced Materials, 2018, 30, e1706285.	21.0	26
57	Microstructure and morphology evolution in chemical solution deposited semiconductor films: 2. PbSe on As face of GaAs(111). EPJ Applied Physics, 2004, 28, 51-57.	0.7	25
58	Real Time Monitoring of the Deposition Mechanism in Chemical Solution Deposited PbSe Films Using Light Scattering. Chemistry of Materials, 2006, 18, 3593-3595.	6.7	25
59	Frictional Properties of Surfactant-Coated Rod-Shaped Nanoparticles in Dry and Humid Dodecane. Journal of Physical Chemistry B, 2008, 112, 14395-14401.	2.6	25
60	In situ monitoring the role of citrate in chemical bath deposition of PbS thin films. CrystEngComm, 2016, 18, 149-156.	2.6	25
61	Transmission electron microscopy of epitaxial PbS nanocrystals on polydiacetylene Langmuir films. Nanotechnology, 2004, 15, S316-S321.	2.6	24
62	Chemically Programmed Ultrahigh Density Two-Dimensional Semiconductor Superlattice Array. Journal of the American Chemical Society, 2010, 132, 1212-1213.	13.7	24
63	Zinc modified polydiacetylene Langmuir films. Soft Matter, 2011, 7, 9069.	2.7	24
64	Chemical bath deposited PbS thin films on ZnO nanowires for photovoltaic applications. Thin Solid Films, 2014, 550, 149-155.	1.8	24
65	Phonon band gaps in the IV-VI monochalcogenides. Physical Review B, 2019, 100, .	3.2	24
66	Generic Substrate for the Surface Forces Apparatus:Â Deposition and Characterization of Silicon Nitride Surfaces. Langmuir, 2000, 16, 6955-6960.	3.5	23
67	Enhanced photoluminescence and photonic bandgap modification from composite photonic crystals of macroporous silicon and nanocrystalline PbS thin films. Applied Physics Letters, 2008, 93, 073111.	3.3	23
68	The x-ray surface forces apparatus for simultaneous x-ray diffraction and direct normal and lateral force measurements. Review of Scientific Instruments, 2002, 73, 2486-2488.	1.3	22
69	Microstructure and morphology evolution in chemical solution deposited semiconductor films: 3. PbSe on GaAs vs. Si substrate. EPJ Applied Physics, 2005, 31, 27-30.	0.7	22
70	Chemical solution deposited PbS thin films on Si(100). Physica Status Solidi C: Current Topics in Solid State Physics, 2008, 5, 3431-3436.	0.8	22
71	Electrodeposited quantum dots IV. Epitaxial short-range order in amorphous semiconductor nanostructures. Surface Science, 1996, 350, 277-284.	1.9	21
72	Normal and Shear Forces Generated during the Ordering (Directed Assembly) of Confined Straight and Curved Nanowires. Nano Letters, 2008, 8, 246-252.	9.1	21

YUVAL GOLAN

#	Article	IF	CITATIONS
73	Surface Termination Control in Chemically Deposited PbS Films: Nucleation and Growth on GaAs(111)A and GaAs(111)B. Journal of Physical Chemistry C, 2011, 115, 16501-16508.	3.1	21
74	CuS Nanoparticle Additives for Enhanced Ester Lubricant Performance. ACS Applied Nano Materials, 2018, 1, 7060-7065.	5.0	21
75	Effect of carbon implantation on visible luminescence and composition of Si-implanted SiO2 layers. Surface and Coatings Technology, 2009, 203, 2658-2663.	4.8	20
76	Electrodeposited quantum dots: Coherent nanocrystalline cdse on oriented polycrystalline au films. Advanced Materials, 1997, 9, 236-238.	21.0	19
77	Strengthening of poly-crystalline (ceramic) Nd:YAG elements for high-power laser applications. Optical Materials, 2011, 33, 695-701.	3.6	19
78	Effect of Metal Cations on Polydiacetylene Langmuir Films. Langmuir, 2012, 28, 4248-4258.	3.5	18
79	Surface plasmon resonance in surfactant coated copper sulfide nanoparticles: Role of the structure of the capping agent. Journal of Colloid and Interface Science, 2015, 457, 43-51.	9.4	18
80	Vacuumâ€Deposited Gold Films: II . Role of the Crystallographic Orientation of Oxideâ€Covered Silicon Substrates. Journal of the Electrochemical Society, 1995, 142, 1629-1633.	2.9	17
81	Template Growth of Nanocrystalline PbS, CdS, and ZnS on a Polydiacetylene Langmuir Film: An In Situ Grazing Incidence X-ray Diffraction Study. Advanced Functional Materials, 2006, 16, 2398-2404.	14.9	17
82	Hierarchical superstructure of alkylamine-coated ZnS nanoparticle assemblies. Physical Chemistry Chemical Physics, 2011, 13, 4974.	2.8	17
83	Oriented Attachment: A Path to Columnar Morphology in Chemical Bath Deposited PbSe Thin Films. Crystal Growth and Design, 2018, 18, 1227-1235.	3.0	17
84	Chemical epitaxy of π-phase cubic tin monosulphide. CrystEngComm, 2020, 22, 6170-6181.	2.6	17
85	Substrate Reactivity and "Controlled Contamination―in Metalorganic Chemical Vapor Deposition of GaN on Sapphire. Japanese Journal of Applied Physics, 1998, 37, 4695-4703.	1.5	16
86	Enhanced SWIR absorption in chemical bath deposited PbS thin films alloyed with thorium and oxygen. RSC Advances, 2016, 6, 88077-88084.	3.6	16
87	Electric Response of CuS Nanoparticle Lubricant Additives: The Effect of Crystalline and Amorphous Octadecylamine Surfactant Capping Layers. Langmuir, 2019, 35, 15825-15833.	3.5	16
88	The effect of complexing agents in chemical solution deposition of metal chalcogenide thin films. Materials Chemistry Frontiers, 2021, 5, 2035-2050.	5.9	16
89	Tunability of the optical band edge in thin PbS films chemically deposited on GaAs(100). Journal of Physics Condensed Matter, 2010, 22, 262002.	1.8	15

90 The role of interparticle and external forces in nanoparticle assembly. , 2009, , 38-49.

14

#	Article	IF	CITATIONS
91	Enhanced photoluminescence from GaN grown by lateral confined epitaxy. Journal of Applied Physics, 2002, 91, 1191-1197.	2.5	13
92	Chemical deposition and characterization of thorium-alloyed lead sulfide thin films. Thin Solid Films, 2014, 556, 223-229.	1.8	13
93	Chemical epitaxy of CdSe on GaAs. CrystEngComm, 2017, 19, 5381-5389.	2.6	13
94	Surface energies and nanocrystal stability in the orthorhombic and π-phases of tin and germanium monochalcogenides. CrystEngComm, 2018, 20, 4237-4248.	2.6	13
95	Layer-by-layer growth in solution deposition of monocrystalline lead sulfide thin films on GaAs(111). Materials Chemistry Frontiers, 2019, 3, 1538-1544.	5.9	13
96	Photoluminescence of polydiacetylene membranes on porous silicon utilized for chemical sensors. Optical Materials, 2008, 30, 1766-1774.	3.6	12
97	Effect of hot acid etching on the mechanical strength of ground YAG laser elements. Journal of Physics and Chemistry of Solids, 2008, 69, 839-846.	4.0	12
98	Thermal healing of the sub-surface damage layer in sapphire. Materials Chemistry and Physics, 2010, 124, 323-329.	4.0	12
99	Citrate-controlled chemical solution deposition of PbSe thin films. CrystEngComm, 2019, 21, 1818-1825.	2.6	12
100	Stability of cubic tin sulphide nanocrystals: role of ammonium chloride surfactant headgroups. Nanoscale, 2019, 11, 17104-17110.	5.6	12
101	â€~Beneficial impurities' in colloidal synthesis of surfactant coated inorganic nanoparticles. Nanotechnology, 2021, 32, 102001.	2.6	12
102	Skeletal architecture and microstructure of the calcifying coral Fungia simplex. Materials Science and Engineering C, 2003, 23, 473-477.	7.3	11
103	Optical properties of size quantized PbSe films chemically deposited on GaAs. EPJ Applied Physics, 2008, 41, 75-80.	0.7	11
104	Two-Photon Polymerization of Polydiacetylene. Journal of Physical Chemistry B, 2009, 113, 1273-1276.	2.6	11
105	Hetero-Twinning in Chemical Epitaxy of PbS Thin Films on GaAs Substrates. Crystal Growth and Design, 2012, 12, 4006-4011.	3.0	11
106	Microstructure related transport phenomena in chemically deposited PbSe films. Materials Chemistry and Physics, 2008, 112, 132-135.	4.0	10
107	Chemical epitaxy of CdS on GaAs. Journal of Materials Chemistry C, 2017, 5, 1660-1667.	5.5	10
108	Mapping Charge Distribution in Single PbS Core – CdS Arm Nano-Multipod Heterostructures by Off-Axis Electron Holography. Nano Letters, 2017, 17, 2778-2787.	9.1	10

#	Article	IF	CITATIONS
109	High photoconductive gain in a GaAs/PbS heterojunction based SWIR detector. Applied Physics Letters, 2020, 117, .	3.3	10
110	Cathodoluminescence study of micro-crack-induced stress relief for AlN films on Si(111). Journal of Electronic Materials, 2006, 35, L15-L19.	2.2	9
111	Phase transformation of PbSe/CdSe nanocrystals from core-shell to Janus structure studied by photoemission spectroscopy. Physical Review B, 2013, 87, .	3.2	9
112	Beneficial Impurities and Phase Control in Colloidal Synthesis of Tin Monoselenide. Langmuir, 2019, 35, 15855-15863.	3.5	9
113	Morphology control of perovskite films: a two-step, all solution process for conversion of lead selenide into methylammonium lead iodide. Materials Chemistry Frontiers, 2021, 5, 1410-1417.	5.9	9
114	Electrodeposited Quantum Dots. 6. Epitaxial Size Control in Cd(Se, Te) Nanocrystals on {111} Gold. Israel Journal of Chemistry, 1997, 37, 303-313.	2.3	8
115	Two―and threeâ€dimensional composite photonic crystals of macroporous silicon and lead sulfide semiconductor nanostructures. Physica Status Solidi (A) Applications and Materials Science, 2009, 206, 1290-1294.	1.8	8
116	Nanometer size effects in nucleation, growth and characterization of templated CdS nanocrystal assemblies. Nanoscale, 2012, 4, 7655.	5.6	8
117	The effect of short chain thiol ligand additives on chemical bath deposition of lead sulphide thin films: the unique behaviour of 1,2-ethanedithiol. CrystEngComm, 2016, 18, 9122-9129.	2.6	8
118	Infrared photoconductivity and photovoltaic response from nanoscale domains of PbS alloyed with thorium and oxygen. Nanotechnology, 2018, 29, 115202.	2.6	8
119	Effect of light regimes on the microstructure of the reef-building coral Fungia simplex. Materials Science and Engineering C, 2005, 25, 81-85.	7.3	7
120	Twinning and Phase Control in Template-Directed ZnS and (Cd,Zn)S Nanocrystals. Crystal Growth and Design, 2013, 13, 2149-2160.	3.0	7
121	Chemical, structural and photovoltaic properties of graded CdS _x Se _{1â^'x} thin films grown by chemical bath deposition on GaAs(100). CrystEngComm, 2018, 20, 5735-5743.	2.6	7
122	Chemical epitaxy and interfacial reactivity in solution deposited PbS on ZnTe. Journal of Materials Chemistry C, 2016, 4, 1996-2002.	5.5	6
123	Electrical and optical characterization of extended SWIR detectors based on thin films of nano-columnar PbSe. Infrared Physics and Technology, 2019, 96, 89-97.	2.9	6
124	In situ X-ray Diffraction Studies of a Multilayered Membrane Fluid under Confinement and Shear. International Journal of Thermophysics, 2001, 22, 1175-1184.	2.1	5
125	Interfacial characterization of chemical solutionâ€deposited thin films of PbSe on GaAs(100). Surface and Interface Analysis, 2008, 40, 939-943.	1.8	5
126	Compositional tunability in solid solution PbS _x Se _{1â^'x} thin films chemically deposited on GaAs(100). CrystEngComm, 2015, 17, 3433-3439.	2.6	5

#	Article	IF	CITATIONS
127	A New Solid Solution Approach for the Study of Self-Irradiating Damage in non-Radioactive Materials. Scientific Reports, 2017, 7, 2780.	3.3	5
128	Postgrowth Control of the Interfacial Oxide Thickness in Semiconductor–Insulator–Semiconductor Heterojunctions. Advanced Materials Interfaces, 2018, 5, 1800231.	3.7	5
129	Liquid flow deposition of PbS films on GaAs(100). CrystEngComm, 2018, 20, 3765-3771.	2.6	5
130	Chemical epitaxy of a new orthorhombic phase of Cu2â^'xS on GaAs. CrystEngComm, 2019, 21, 6063-6071.	2.6	5
131	A new binary phase in the tin monoselenide system: chemical epitaxy of orthorhombic γ-SnSe thin films. Materials Chemistry Frontiers, 2021, 5, 5004-5011.	5.9	5
132	Formation of Ge Nanocrystals in Al ₂ O ₃ Matrix. Journal of Nanoscience and Nanotechnology, 2008, 8, 759-763.	0.9	4
133	Luminescence and structure of nanosized inclusions formed in SiO2 layers under double implantation of silicon and carbon ions. Journal of Surface Investigation, 2009, 3, 702-708.	0.5	4
134	Directed Coassembly of Oriented PbS Nanoparticles and Monocrystalline Sheets of Alkylamine Surfactant. Langmuir, 2012, 28, 15119-15123.	3.5	4
135	Time, illumination and solvent dependent stability of cadmium sulfide nanoparticle suspensions. Journal of Colloid and Interface Science, 2014, 430, 283-292.	9.4	4
136	A Two-Step, All Solution Process for Conversion of Lead Sulfide to Methylammonium Lead Iodide Perovskite Thin Films. Thin Solid Films, 2020, 714, 138367.	1.8	4
137	The role of CdS doping in improving SWIR photovoltaic and photoconductive responses in solution grown CdS/PbS heterojunctions. Nanotechnology, 2020, 31, 255502.	2.6	4
138	Sample preparation induced phase transitions in solution deposited copper selenide thin films. RSC Advances, 2021, 12, 277-284.	3.6	4
139	Substrate Surface Treatments and "Controlled Contamination―in GaN / Sapphire MOCVD. Materials Research Society Symposia Proceedings, 1997, 482, 157.	0.1	3
140	Microstructure of GaN deposited by lateral confined epitaxy on patterned Si (111). Journal of Electronic Materials, 2002, 31, 88-93.	2.2	3
141	High-quality GaN on intentionally roughened c-sapphire. EPJ Applied Physics, 2003, 22, 11-14.	0.7	3
142	Thermochemical strengthening of Nd:YAG laser rods. , 2006, , .		3
143	Structural and Optical Properties of Al2O3 with Si and Ge Nanocrystals. Materials Research Society Symposia Proceedings, 2006, 958, 1.	0.1	3
144	Silicon Photonic Crystals Doped with Colloidally Synthesized Lead Salt Semiconductors Nanocrystals. Journal of Nanoscience and Nanotechnology, 2009, 9, 3648-3651.	0.9	3

#	Article	IF	CITATIONS
145	Studying of quantum-size effects origination in semiconducting lead sulfide nanocrystals. Protection of Metals and Physical Chemistry of Surfaces, 2010, 46, 633-638.	1.1	3
146	Complex investigation of electronic structure transformations in Lead Sulphide nanoparticles using a set of electron spectroscopy techniques. Vacuum, 2012, 86, 638-642.	3.5	3
147	Architecture, development and implementation of a SWIR to visible integrated up-conversion imaging device. Proceedings of SPIE, 2016, , .	0.8	3
148	Combinatorial Liquid Flow Deposition of PbS Semiconductor Thin Films. Industrial & Engineering Chemistry Research, 2021, 60, 15593-15599.	3.7	2
149	Optoelectronic Characterization of Epitaxial Films of Electrodeposited CdSe Quantum Dots. , 1996, , 579-590.		1
150	Microstructure of GaN grown by lateral confined epitaxy 2. GaN on patterned sapphire. Journal of Electronic Materials, 2003, 32, 23-28.	2.2	1
151	A qualitative description of preferred orientation in porous carbonate matrices of marine origin. Materials Science and Engineering C, 2003, 23, 593-595.	7.3	1
152	Reduction of oxygen contamination in AlN. Physica Status Solidi C: Current Topics in Solid State Physics, 2003, 0, 2541-2544.	0.8	1
153	Composite photonic crystal cavities of macro porous silicon and lead sulfide thin films. Physica Status Solidi (A) Applications and Materials Science, 2011, 208, 1394-1398.	1.8	1
154	Morphology control in chemical solution deposited lead selenide thin films on fluorine-doped tin oxide. Thin Solid Films, 2020, 710, 138256.	1.8	1
155	NMR and EPR study of cubic ï€-phase SnS semiconductor nanoparticles. Materials Chemistry and Physics, 2020, 250, 123206.	4.0	1
156	On the "Chemical Inertness―of Teflon in Chemical Synthesis. Industrial & Engineering Chemistry Research, 2021, 60, 11995-12000.	3.7	1
157	The Role of Semiconductor/Substrate Mismatch in the Formation of Electrodeposited Quantum Dots. , 1996, , 167-174.		1
158	Electroless Deposited Nickel Thin Films Alloyed with Thorium. Crystal Research and Technology, 0, , 2100194.	1.3	1
159	Electron spectroscopy investigations of semiconductor nanocrystals formed by various technologies. International Journal of Nanoparticles, 2008, 1, 14.	0.3	0
160	Monochalcogenide Semiconductors: Ï€â€Phase Tin and Germanium Monochalcogenide Semiconductors: An Emerging Materials System (Adv. Mater. 41/2018). Advanced Materials, 2018, 30, 1870310.	21.0	0
161	The effect of deposition mechanism on the properties of epitaxial PbS films grown from acidic bath. Materials Chemistry Frontiers, 2021, 5, 2860-2866.	5.9	0
162	Amidation-Controlled Polymorphism in SnS Nanoparticles. Crystal Growth and Design, 0, , .	3.0	0